Original Article
DOI: 10.4274/tjps.galenos.2021.62333

Cocrystal Construction Between Rosuvastatin Calcium and L-asparagine with Enhanced Solubility and Dissolution Rate

Venkata Deepthi Vemuri[1]*, Srinivas Lankalapalli [2]
[1]Maharajah's College of Pharmacy, Phool Baugh, Vizianagaram-535002, India
[2]GITAM Institute of Pharmacy, GITAM (Deemed to be University), Visakhapatnam, Andhra Pradesh, INDIA

Corresponding author:
Corresponding author: Venkata Deepthi Vemuri*
Mailing address: Maharajah's College of Pharmacy, Phool Baugh, Vizianagaram-535002, Andhra Pradesh, India
Mobile phone: +91-9032292387
E-mail: deepthichowdary438@gmail.com
https://orcid.org/0000-0003-3243-4340
20.12.2020
03.04.2021

Abstract
Background: Rosuvastatin calcium, a synthetic BCS class-II drug with low solubility and high permeability utilized in hyperlipidaemia management. In the present investigation, an attempt was made towards the modification of the physicochemical properties of rosuvastatin calcium by applying crystal engineering to prepare a cocrystal form. Cocrystals of rosuvastatin calcium with GRAS status co-former L-Asparagine were prepared by utilizing solvent evaporation method.
Result: The Obtained cocrystals was evaluated by Fourier transform infrared spectroscopy, powder X-ray diffraction, FT-Nuclear magnetic resonance spectroscopy, Scanning electron microscopy, and differential scanning calorimetry. Powder X-ray diffraction studies revealed the presence of unique crystalline peaks, which provides the interaction details of API and the co-former. The changes in the thermal behaviour of cocrystals were confirmed by differential scanning calorimetry studies. Alteration in the chemical shift values of FT-NMR at OH group confirms the hydrogen bond interaction between drug and co-former. Comparative studies on the solubility and dissolution rate were conducted and exhibited an almost 2-fold higher than the parent drug.
Conclusion: A new co-crystal form of rosuvastatin calcium was obtained with enhanced solubility and dissolution rate than the parent drug, which encloses new circumstances for use of these cocrystals
Keywords: Cocrystals, Rosuvastatin calcium, Solubility, Dissolution, Solvent evaporation co-crystallization.

Article Highlights:
- Novel cocrystals of rosuvastatin calcium prepared with biologically accepted amino acids as co-formers.
- Characterization of cocrystals was done by FTIR, powder X-ray diffraction, differential scanning calorimetry, ^{1}H liquid NMR, and scanning electron microscopy.
- In vitro characterization of cocrystals by solubility and dissolution drug release.
- Modulated chemical environment and Improved the solubility of parent molecule by co-crystallization technique by using synthon approach.

1. Background

In modern investigations like hybrid liquisolid systems, solid dispersions along with cocrystals have emerged in the evolution of supramolecular systems [1,2]. The procreation of supramolecules with intend to structure and distinct physicochemical properties is the overturn of crystal engineering. Cocrystals are cognominated among the products that are obtained from the crystal engineering approach with ionic/non-covalent intermolecular interaction between two or more disparate molecules with a certain stoichiometric ratio in a crystal lattice [3,4] at most one molecule should be active moiety. Generally, the choice of co-former should be done from GRAS (Generally recognized as safe) or EAFUS (Everything added to food in united states) list, which frequently without pharmacological efficacy [5,6]. Therefore, it contributes a practical approach in organizing the physicochemical properties with no medical efficacy diversity [7,8]. Over the past few decades, many of the literature revealed that there is a great rise in the utilization of the co-crystallization approach and their feasible usage in the formulation as an optimized approach for modulating physicochemical and biopharmaceutical properties of active moiety [9,10].

Rosuvastatin calcium (RSC) is a synthetic BCS class-II molecule utilized in hyperlipidemia management by enhancing HDL cholesterol and by lowering triglycerides, LDL cholesterol, and apolipoprotein. It can be utilized to decreasing the furtherance of atherosclerosis and capable for the avoidance of coronary heart diseases [11]. Rosuvastatin has accomplished fair outcomes in the potency and safety conditions, accepted as "super statin" [12,13]. Rosuvastatin exhibits low water solubility (0.33 mg/ml) due to its crystalline nature [14,15] which displays low solubility in gastrointestinal Fluids. The oral bioavailability of RSC is about 20% due to pervasive first-pass hepatic biotransformation [16] and greater doses were combined with elevated occurrence of haematuria, proteinuria, elevated serum creatinine, and rhabdomyolysis [17].

Co-crystallization of RSC may endeavor a possible formulation path to enhance the bioavailability of molecules outside changing the chemical integrity and upholding the physical stability. Cocrystals of RSC with co-formers like sorbitol [18], vanillin [19] has been generated with improved bioavailability and contributing embellished feasibility to modulate and design better drug product [20]. Ferrori et al., 2014 in his patent [21] described the methods for the preparation of RSC by utilizing three RSC cocrystals such as Rosuvastatin 2-aminopyrimidine hemihydrate, Rosuvastatin pyrazine hydrate, and Rosuvastatin quinoxaline.

The selection of co-former in most cases should be based on Cambridge structural database (CSD), functional/structural possessions, and should be mentioned as risk-free (GRAS status) [22,23]. The co-former selected should essentially carry a group able to develop molecular synthons with the active moiety. In this Framework, amino acids appear to be a beneficial option as an applicable companion. Amino acids exist under the GRAS group, besides pretty low toxicity and inexpensive. Many of the salt, that is formed from the amino acids with various classes of therapeutic agents were reported in previous literatures [24,25].

The aspiration of the present investigation was to develop cocrystals of RSC with the GRAS group of co-former L-asparagine (ASN) by utilizing the solvent evaporation method to modulate the physicochemical properties of the molecule. The molecular structures of RSC and ASN were shown in Fig. 1. The obtained cocrystals were characterized by powder x-ray diffraction, IR spectroscopy, scanning electron microscopy, and differential scanning calorimetry. In vitro studies like apparent solubility studies, dissolution studies and stability studies were conducted and compared between RSC and its cocrystals.

2. Methods:

2.1 Materials

Rosuvastatin calcium was obtained as a gift sample from Apex laboratory pvt ltd, Chennai. L-asparagine and methanol (chromatographic grade) were purchased from Lotus chemicals (Andhra Pradesh, India). All the chemicals used in the study were analytical reagent grade.

2.2 Co-former selection

In the formation of co-crystals, amino acids, perhaps be of initial attraction. Furthermore, their zwitterionic potential is capable of forming zwitterionic cocrystals [26,27]. A Tilborg in his minireview [27] provided the list of amino acids that signify the formation of cocrystals based on CSD [28], structural research, and the Scifinder literature scanning program, which may be helpful for many of the researches in the selection of suitable amino acids as a co-former. Based on his examination L-asparagine does not carry any controversial side chains, allowing to be under zwitterionic state and to produce cocrystals [29]. Considering the safety and effectiveness in the preparation of the cocrystals, the stoichiometric ratio of the drug and co-former was selected for the present investigation.

2.3 Rosuvastatin-L-Asparagine Cocrystal synthesis

The stoichiometric ratio of RSC (150mg) and L-Asparagine (42mg) was dissolved in 5 ml of methanol and 1.5 ml of water separately to form a clear solution with the help of sonicator. Both the solutions were mixed and placed on a magnetic stirrer with 900rpm. The stirring process is continued until the solvent is evaporated completely at room temperature. The obtained cocrystals were washed with methanol: water (5:1) for 3-5 times and filtered through the membrane filter (pore size 0.45µm), to ensure the removal of unbound drug and the co-former. The resulting product was placed in a desiccator overnight. The solvent evaporation method was utilized to produce large scale samples for evaluation.

2.4 Aqueous solubility studies

Solubility analysis was conducted in distilled water, pH 1.2 buffer, pH 4.5 buffer, and pH 6.8 phosphate buffer solution. Excess amount of RSC (approx. 50mg) and RSC-ASN cocrystals (RSC-C) (Eq. wt. to 50mg of pure RSC) were added each in screw-capped vials containing 10 ml of distilled water and pH 6.8 phosphate buffer with continuous stirring for 48h in water bath shaker. This was maintained at 37°C with 200rpm and filtered through a 0.45µ membrane filter. The quantitative analysis of RSC in the filtrate was done spectrophotometrically using UV-Spectrophotometer (V-630, Jasco, Japan) at 244nm. All the equilibrium analysis was conducted in triplicate and the residual solvents were centrifuged and subjected to FTIR.

2.5 In vitro dissolution studies

In vitro dissolution of RSC and the obtained cocrystals were determined by using 900 ml of pH 6.8 phosphate buffer at 37°C and 50rpm as per USP. This was performed using USP apparatus-I dissolution vessel (TDL-08L, Electrolab, India). The highest dose of RSC (40mg) and cocrystals (Eq. wt. of RSC 40 mg) each was weighed

and the intact powder was placed in dissolution vessel. 5ml of the samples were collected at selected time periods of 0, 10, 20, 30, 40, 50, and 60 min and replenished with fresh buffer. The drug content in the filtered sample was measured spectrophotometrically using UV spectrophotometer (V-630, Jasco, Japan).

2.6 Powder x-ray diffraction

PXRD pattern analysis of RSC, ASN, and obtained cocrystals were done by XRD Diffractometer (powder) Philips Xpert MPD (Philips, Holland). The instrument was equipped with a Cu target X-Ray tube source and Xe-filled counteract or proportional detector. The diffraction data was collected by maintaining tube voltage and tube current at 30kV and 15mA respectively for 2 theta scan axis, scan ranging from 5 to 65° with a step width of 0.02° and a scan speed of 10.00°/min. JCPDF database software was used to determine peak intensity for each sample.

2.7 Fourier transform infrared spectroscopy

Infrared absorption spectra of all the samples were obtained by utilizing FT-IR Azilent carry 360 series containing DLATGS detector with $2cm^{-1}$ spectra resolution. Approximately 2 to 4mg of the powdered sample was placed in the sample cell and scanned over 4000 - $400cm^{-1}$ and the data obtained were analyzed with OPUS spectral software.

2.8 Scanning electron microscope

Surface images of pure drug RSC, co-former ASN, and the obtained cocrystals were acquired at various magnifications by utilizing scanning electron microscope XL30ESEM with EDAX equipped with secondary and backscattered electron detector. Samples were prepared for SEM analysis by attaching to carbon tabs, placed on the aluminium pin stubs and sputter-coated with gold/palladium under vacuum.

2.9 Differential scanning calorimeter

Differential scanning calorimeter measurements of all the samples were obtained by utilizing Mettler Teledo DSC 821e instrument under nitrogen purge (30ml/min). 2-5 mg of powder sample was loaded into aluminium pans and sealed. Scanning of samples was done from 30°C to 350°C at a heating rate of 10°C/min. TAQ series advantage software was used for the data collection.

2.10 ^{1}H liquid FT-NMR Spectroscopy:

The pure drug RSC and RSC-C co-crystals were dissolved in deuterated dimethyl sulfoxide and the conformer ASN was dissolved in deuterated water for FT-NMR analysis. ^{1}H FT-NMR spectra of RSC, ASN, and RSC-C co-crystals were recorded in 400 MHz FT-NMR spectrometer (model: JNM- ECz 400S) and chemical shifts were observed.

2.11 Product Yield and Drug Content Estimation:

The prepared cocrystals were collected and weighed accurately, the product yield was calculated by dividing the actual weight of obtained cocrystals to that of the total weight of drug and the co-former.

$$\text{Percentage yield} = \frac{Weight\ of\ cocrystals}{Total\ weight\ of\ drug\ and\ coformer} \times 100 \quad (1)$$

Prepared cocrystals were accurately weighed equivalent to 100mg of pure drug and dissolved in 100 ml of pH 6.8 phosphate buffer. The solution was filtered and analysed for drug content using UV-Visible spectrophotometer at 244nm.

2.12 Micromeritic evaluation of Cocrystals

Micromeritic properties of RSC-C cocrystals were compared with pure drug RSC. Both RSC and RSC-C were characterized for bulk density, tapped density, Hausner ratio, Carr's index and angle of repose. USP method I was utilized for determination of bulk density, whereas USP method II with tapped density tester (Aymes, Turkey) was utilized to determine tapped density. Following equations were utilized for calculation of Hausner ratio, Carr's index and angle of repose.

Hausner ratio = tapped density/bulk density (2)

*Carr's index % = (tapped density – bulk density)*100/tapped density* (3)

$Tan\ \Theta = 2h/D$ (4)

3. Results

3.1 Aqueous solubility analysis

Solubility analysis was conducted in distilled water, pH 1.2 buffer, pH 4.5 buffer, and pH 6.8 phosphate buffer solution. Pure RSC exhibited 0.836 mg/ml, 0.624 mg/ml, 1.143 mg/ml, and 1.427 mg/ml concentration in water pH 1.2 buffer, pH 4.5 buffer, and pH 6.8 phosphate buffer respectively at 48h with continuous stirring. RSC-ASN physical mixture has no significant difference in the solubility when compared to pure API. RSC-C cocrystals exhibited 2.17-fold enhancement of solubility in water, 2.21-fold in pH 1.2 buffer, 2.29-fold in pH 4.5 buffer, whereas 2.42-fold high in pH 6.8 phosphate buffer when compared to pure RSC (Table 1). The possibilities of these outcomes are the crystal arrangement and the co-crystallization process [30]. As RSC is poorly water soluble [14,15], the cocrystal solubility greatly relies upon the solubility of its composition [31]. Small particle size might be the additional reason for the improved solubility when compared to pure RSC. This establishes the possibility of RSC-C cocrystals to sight for new productive formulation.

3.2 PXRD analysis:

The diffractogram pattern of RSC-C cocrystals exhibited unique crystalline peaks when related to RSC and the co-former. The PXRD pattern of pure drug, co-former, and the obtained cocrystals were shown in Fig. 2. Pure RSC showed single 2Θ scattering angle at 43.25° indicating the amorphous nature of the drug [32]. RSC-C cocrystals showed new characteristic peaks at 9.14°, 10.28°, 20.85°, 24.61°, 32.93°, and 40.06° which were absent in diffractogram pattern of pure RSC and ASN. Whereas, 11.85°, 17.70°, 18.23°, 19.91°, 27.84°, and 43.15° peaks of ASN shifted to 11.71°, 17.53°, 18.05°, 19.73°, 27.72°, and 42.46° respectively in the cocrystals. The appearance disappearance and shifting of the peaks in the diffractogram pattern of cocrystals when compared with pure drug and co-former indicates the evaluation of a new crystalline phase.

3.3 FTIR Studies:

The interaction between RSC and ASN was demonstrated by utilizing FTIR spectroscopic technique. The FTIR spectra of RSC show characteristic peaks referring to carboxylic O-H stretch at 3382 cm^{-1}, N-H stretch at 2968 cm^{-1}, C=C stretch at 1541 cm^{-1}, asymmetric vibration of CH_3 at 1436 cm^{-1}, C-F stretch at 1149 cm^{-1}, symmetric vibration of CH_3 at 1379 cm^{-1}, and C-H plane bending of aromatic ring at 775 cm^{-1} [33]. For ASN, characteristic peaks ponding to O-H stretch at 3436 cm^{-1}, N-H stretch at 2924, and C=O stretch at 1716-1750 [34].

The infra-red spectra of RSC, ASN, cocrystals RSC-C were shown in Fig. 3. When compared with the pure RSC, the N-H group shifts to 2931cm^{-1} and the O-H shifts to 3421cm^{-1} remarkably displaying new hydrogen bond generation in cocrystals. In inclusion to the characteristic peaks of RSC few adding peaks were noticed in the range of 1638 – 1750 cm^{-1} due to the carboxylic acid moiety which expresses the presence of C=O stretching in cocrystals. Alter in the chemical environment was observed in the cocrystals when compared with the pure RSC, this was consistent with those demonstrated by PXRD and DSC results and affirm the interaction between RSC and ASN.

3.4 SEM analysis:

Field emission scanning electron microscopy (SEM) micrographs of RSC, ASN, and RSC-C cocrystals obtained from solvent evaporation were shown in the Fig. 4. Rosuvastatin Calcium presented irregular granular shaped particles, there is no much alteration between the morphology of pure RSC and RSC-ASN physical mixture. Asparagine exhibited stick-shaped crystalline morphology. The co-crystals obtained from solvent evaporation exhibited phenomenal change into irregular closely fitted crystalline structure. The incident might be the establishment of intermolecular hydrogen bonds between RSC and ASN.

3.5 DSC analysis:

DSC data of RSC-C cocrystals were obtained and compared with pure drug and the co-former shown in Fig. 5. DSC thermogram of pure drug RSC showed the broad endothermic peak at 80.7°C and 217.9°C indicating the amorphous form of drug substance [35]. The thermal curve of ASN exhibited a sharp endothermic peak at 116.1°C and 237.1°C with high enthalpy. Physical mixture (1:1 ratio) with RSC and ASN presented endothermic peaks at 101.8°C and 237.1°C with slight shifting and broadening of peaks, this may be due to the loss of purity of each compound when mixed together and not a fundamental indication of incompatibility. It was noticed that the RSC-C cocrystal obtained by solvent evaporation presented a unique characteristic sharp endothermic peak at 127°C with high intensity which was different from pure RSC and ASN co-former. According to many researchers, most of the cocrystals melt at the temperature that is different from their API and co-former. Based on the Perlovich study, normally the melting points of the obtained cocrystals are in the middle (55.3%), less (38.9%), and high (14.5%) to that of starting materials [36]. RSC-C cocrystals exhibited middle endotherm when compared to starting materials on DSC profile, which is a very common phenomenon of 1:1 stoichiometric cocrystals. Change in the melting point indicates the modification in the crystalline structure and cocrystal formation. This change was evidenced by PXRD and FT-IR analysis.

3.6 ^{1}H liquid FT-NMR Spectroscopy:

The ^{1}H FT-NMR spectra of RSC, ASN, and RSC-C co-crystals were shown in Fig. 7. On comparing NMR spectra of RSC-C co-crystals with pure drug (RSC) spectra, changes in the chemical shift values were observed at 3H from 3.395 to 3.428 and and 6H from 3.500 to 3.533 respectively. This chemical shift value alteration confirmed the co-crystal formation between drug and the co-former probably due to the interaction of free hydroxyl group of RSC with the amine moiety of the ASN. Furthermore, the outcomes attained by FT-NMR analysis were in agreement with DSC, PXRD, and FT-IR analysis.

3.7 In vitro dissolution analysis

The cumulative dissolution rate was determined to pure RSC and RSC-C cocrystals obtained by solvent evaporation. The dissolution rate was carried out in pH 6.8 buffer and was presented in Fig. 7. Immediately after the addition of solvent, RSN showed 0.86% of dissolution rate whereas RSC-C cocrystal presented 3.8%. After 10 minutes, the dissolution rate of cocrystals was enhanced to 23.23% while pure drug presented 9.42 % of dissolution. Pure RSC showed a slow enhancement in dissolution and reached 42.64% within 2h, in the case of cocrystals there is a sharp increase of dissolution rate and showed 91.02% within 2h. The enhancement on the dissolution of RSC-C cocrystals is due to change in crystal morphology as well as tiny particle size as shown in SEM analysis [37]. Greater dissolution is evidenced with a change in melting point of DSC profile [38,39].

Altered dissimilarity in the cocrystal properties related to pure API were acknowledged in FTIR, PXRD, SEM, DSC, solubility and dissolution analysis are due to alteration in crystalline structure.

3.8 Percentage Yield and Drug Content Estimation

The percentage yield and the drug content estimation of obtained cocrystals were conducted triplicate. The percentage yield of the cocrystals was found to be 95.75 ± 0.25% and the drug content was estimated as 98.4 ± 0.43%. The results indicated the cocrystals obtained showed a good product yield with acceptable drug content.

3.9 Micromeritic evaluation of Cocrystals

The micromeritic properties obtained for both RSC and RSC-C were presented in Table 2. The angle of repose of RSC-C cocrystal was determined to be 29°.81' ± 0.45, whereas for pure RSC it was 32°.31' ± 0.52. This indicates the good flow property of cocrystals in comparison to the pure RSC. The compressibility of cocrystals RSC-C was found to be 6.32 ± 0.68 %, whereas for pure RSC it was 11.24 ± 0.46 %. The result demonstrated excellent compressibility of cocrystals in comparison to pure RSC. The Hauser's of RSC-C and RSC was found to be 1.06 ± 0.02 % and 1.18 ± 0.21, indicating good flow property and strength for compression superior to that of RSC.

4. Discussion

Based on the synthon approach, co-crystal formation mainly depends upon the functional groups that are present in the drug molecule and the co-former [40]. Rosuvastatin consists of two oxydrilic groups bound to asymmetric carbon atoms. So, L-asparagine which contains amide group was selected as a co-former. Thus, the expected structural modification was evidenced by the structural characterization. The results of SEM analysis indicated the conversion of irregular granular nature of pure RSC to closely fitted crystalline structure with in the co-crystals. The RSC-C co-crystals exhibited an average particle size approximate to 4.3µm which is in between the average particle size of pure RSC and ASN. This alteration within the crystalline habit and average particle size might be due to the formation of intermolecular hydrogen bond between drug and the conformer. Alterations in chemical structure by FT-IR in which OH stretching peak at 3382 cm^{-1} was broadened in the RSC-C co-crystals when compared to RSC confirming the hydrogen bond interaction, broad endothermic peak of RSC was altered to sharp endothermic peak in RSC-C co-crystals with different melting point indicating the partial crystallization. Based on Perlovich investigation, 28.9% of the cocrystal formulation exhibited decreased melting point than the parent molecules [41]. The decrease in the melting point and enthalpy indicates the formation of weak crystalline structure [42,43,44]. According to PXRD diffractogram, RSC is in the form of amorphous. Broad peaks in DSC confirms this[45], whereas, RSC-C co-crystal resulted in appearance of new characteristic peaks other than RSC and ASN peaks indicating chemical environment change and change from semi-crystalline form to crystalline form, and ^{1}H liquid FT-NMR showed the exact shift of two oxydrilic group to up-field nature which indicates the transfer of electrons from hydroxyl group during hydrogen bond interaction. All these results together confirm the co-crystal formation between drug and the co-former due to interaction of free hydroxyl group of the drug with amine group of the co-former. Later on, comparative studies on the solubility and dissolution rate were conducted and exhibited an almost 2-fold higher than the parent molecule. All the outcomes of micromeritic properties of cocrystals showed good flow property, compressibility, and strength of compression over RSC this provide an advantage in pelleting and tabletting properties.

5. Conclusion

RSC-C cocrystals were successfully prepared by the solvent evaporation co-crystallization technique. Obtained cocrystals exhibited almost 2-fold enhancement in the solubility and dissolution date than the parent molecule. This shows the removal of obstacles like low solubility and low dissolution on the way of RSC to enter the bloodstream. The formation of a new crystalline form was affirmed by FTIR, powder X-ray diffraction data, and FT-NMR. These results were supported by a change in the melting point in the DSC thermogram compared to the pure RSC and ASN. Considering the enhanced physicochemical properties of RSC, it contributes feasibility for novel formulation. The outcomes of micromeritic properties provide the advantage pelleting and tableting properties, the strategy of converting the idea of cocrystals into the application was well explained in the previous literatures, which may be helpful for process development in the future investigation [46, 47, 48]. However, in the present investigation, the In vivo performance of the cocrystals like Cmax and AUC have not been covered and will be taken up in our next publication. The outcomes clearly indicate the modulation in the chemical structure, solubility enhancement, and dissolution enhancement of RSC through co-crystallization.

Acknowledgment

The Authors are thankful to Maharajah's college of pharmacy, Vizianagaram, Andhra Pradesh and GITAM Deemed to be University, Visakhapatnam for providing the facilities to carry the research work.

6. Abbreviations

GRAS: Generally recognized as safe **EAFUS**: Everything added to food in united states **RSC**: Rosuvastatin calcium **BCS:** Bio-pharmaceutical classification system CSD: Cambridge structural database **ASN**: L-

asparagine **RSC-C**: RSC-ASN cocrystals **PXRD:** Powder x-ray diffraction **FT-IR:** Fourier transform infrared spectroscopy **SEM:** Scanning electron microscope **DSC:** Differential scanning calorimeter **FT-NMR:** FT-Nuclear magnetic resonance spectroscopy.

References:

1. Brus J, Albrecht W, Lehmann F, Geier J, Czernek J, Urbanova M, Kobera L, Jegorov A (2017) Exploring the molecular-level architecture of the active compounds in liquisolid drug delivery systems based on mesoporous silica particles: old tricks for new challenges. Mol Pharm 14:2070–2078.
2. Peer D, Karp JM, Hong S, Farokhzad OC, Margalit R, Langer R (2007) Nanocarriers as an emerging platform for cancer therapy. Nat Nanotechnol 2:751–760.
3. Desiraju GR (2013) Crystal engineering: from molecule to crystal. J Am Chem Soc 135:9952-9967.
4. Duggirala NK, Perry ML, Almarsson Ö, Zaworotko MJ (2016) Pharmaceutical cocrystals: along the path to improved medicines. Chem Comm 52:640-655.
5. Sun CC, Hou H, (2008) Improving mechanical properties of caffeine and methyl gallate crystals by cocrystallization. Cryst Growth Des 8:1575-1579.
6. Tanabe Y, Maeno Y, Ohashi K, Hisada H, Roy A, Carriere J, Heyler R, Fukami T (2019) Screening a trace amount of pharmaceutical cocrystals by using an enhanced nano-spot method. Eur J Pharm Biopharm 136:131-137.
7. Shete A, Murthy S, Korpale S, Yadav A, Sajane S, Sakhare S, Doijad R (2015) Cocrystals of itraconazole with amino acids: screening, synthesis, solid state characterization, in vitro drug release and antifungal activity. J Drug Deliv Sci Tec 28:46-55.
8. Luo Y, Chen S, Zhou J, Chen J, Tian L, Gao W, Zhang Y, Ma A, Li L, Zhou Z (2019) Luteolin cocrystals: characterization, evaluation of solubility, oral bioavailability and theoretical calculation. J Drug Deliv Sci Tec 50:248-254.
9. Friscic T, Jones W (2009) Recent advances in understanding the mechanism of cocrystal formation via grinding. Cryst Growth 9:1621-37.
10. Miroshnyk I, Mirza S, Sandler N (2009) Pharmaceutical co-crystals-an opportunity for drug product enhancement. Expert Opin Drug Deliv 6:333-41.
11. Lennernas H, Fager G (1997) Pharmacodynamics and pharmacokinetics of the HMG-21 CoA reductase inhibitors, similarities and differences. Clin Pharmacokinet 32:403–425.
12. Ballantyne MC, Miller E, Chitra R (2004) Efficacy and safety of rosuvastatin alone and in combination with cholestyramine in patients with severe hypercholesterolemia: A randomized, open-label, plulticenter trial. Clinical Therapeutics 26:1855–1864.
13. Kostapanos SM, Derdemezis SC, Filippatos DT, Milionis JH, Kiortsis ND, Tselepis DA (2008) Effect of rosuvastatintreatment onplasma visfatinlevels in patients with primary hyperlipidemia. European Journal of Pharmacology 578:249–252.
14. Alshora DH, Haq N, Alanazi F K, Ibrahim MA, Shakeel F (2016) Solubility of rosuvastatin calcium in different neat solvents at different temperatures. J Chem Thermodyn 94:230–233.
15. Kulkarni NS, Ranpise NS, Mohan G (2015) Development and evaluation of solid self nano-emulsifying formulation of rosuvastatin calcium for improved bioavailability. Trop J Pharm Res 14:575–582.
16. Martin PD, Warwick MJ, Dane AL, Hill SJ, Giles PB, Phillips PJ (2003) Metabolism, excretion, and pharmacokinetics of rosuvastatin in healthy adult male volunteers. Clinical Therapeutics 25:2822–2835.
17. Adeneye AA, Adeyemi OO, Agbaje EO (2010) Anti-obesity and antihyperlipidaemic effect of Hunteria umbellata seed extract in experimental hyperlipidaemia, J. Ethnopharmacol. 130:307–14.
18. Andreas Hafner, Fritz Blatter, Martin Szelagiewicz, Bernd Siebenhaar (2016) Multicomponent system of rosuvastatin calcumi salt and sorbitol, US 9.249:108 B2
19. Andreas Hafner, Fritz Blatter, Martin Szelagiewicz, Bernd Siebenhaar (2014) Multicomponent crystalline (52) u.s. cl. system of rosuvastatin calcum salt and vanillin. US 8.841:316 B2.
20. Andreas Hafner, Fritz Blatter, Martin Szelagiewicz, Bernd Siebenhaar (2014) Multicomponent crystalline system of rosuvastatin calcum salt and vanillin, US 8.716:305 b2.
21. Clark Ferrari, Andrea Castellin, Marco Galvagni, Nicolas Tesson, Jordi De Mier, Lloreng Rafecas (2014) co-crystal intermediates of rosuvastatin and methods of using same US 8.815:862 b2.
22. Aitipamula A, Velaga S.P, Tan RBH (2010) Formulation of cocrystals from stoichiometric solutions of incongruently saturating systems by spray drying, Cryst. Growth Des. 10:3302-3305.
23. Sarraguca M.C, Ribeiro PRS, Santos AO, Silva MCD, Loppes JA (2014) A PAT approach for the on-line monitoring of pharmaceutical co-crystals formation with near infrared spectroscopy. Int. J Pharm 471:478-484.
24. Inouye S, Iitaka Y (1964) Crystallographic data on the molecular complexes of tetracycline salts. Acta Crystallogr 17:207e208.

25. Rajagopal K, Krishnakumar RV, Nandhini MS, Natarajan S, (2003) L-Histidinium hemihydrochloride tartrate tartaric acid dehydrate. Acta Crystallogr Sect E Struct Rep Online 59:o955eo958.
26. Tilborg A, Springuel G, Norberg B, Wouters J, Leyssens T (2013) Structural study of prolinium/fumaric acid zwitterionic cocrystals: focus on hydrogenbonding pattern involving zwitterionic (ionic) heterosynthons. Cryst Growth Des 13:2373e2389.
27. Tilborg A, Springuel G, Norberg B, Wouters J, Leyssens T (2013) On the influence of using a zwitterionic coformer for cocrystallization: structural focus on naproxeneproline cocrystals. Cryst Eng Comm 15:3341e3350.
28. Allen FH (2002) The Cambridge Structural Database: a quarter million structures and rising, Acta Crystallogr. Sect. B Struct. Crystallogr. Cryst. Chem. 58 380e388.
29. Anaëlle Tilborg, Bernadette Norberg, Johan Wouters (2014) Pharmaceutical salts and cocrystals involving amino acids: A brief structural overview of the state-of-art. Eur J Med Chem 74:411-426.
30. Babu NJ, Nangia A (2011) Solubility advantage of amorphous drugs and pharmaceutical Cocrystals. Cryst Growth Des 7:2662–2679.
31. Good DJ, Rodriguez-Hornedo N (2009) Solubility advantage of pharmaceutical Cocrystals. Cryst Growth Des 5:2252–2264.
32. Beg S, Raza K, Kumar R, Chadha R, Katare OP, Singh B (2016) Improved intestinal lymphatic drug targeting via phospholipid complex-loaded nanolipospheres of rosuvastatin calcium. RSC Adv 6:8173–8187.
33. Mukundkumar Rameshbhai Hirpara , Jyothsna Manikkath, K Sivakumar, Renuka S Managuli, Karthik Gourishetti, Nandakumar Krishnadas, Rekha R Shenoy, Belle Jayaprakash, Chamallamudi Mallikarjuna Rao, Srinivas Mutalik (2017) Long Circulating PEGylated-Chitosan Nanoparticles of Rosuvastatin Calcium: Development and in vitro and in vivo evaluations. Int J Biol Macromol 107:2190-2200.
34. Mäder K, Mehnert W (2001) Solid lipid nanoparticles, production, characterization and applications. Adv Drug Deliv Rev 47:165–196.
35. Elanthiraiyan M, Kandasamy M, Kanagan G, Govindarajan G, Pari S, Sambasivam R (2019) Growth and some Characterization of L-Asparagine Monohydrate Potassium Iodide (LAMPI) Crystals. Compliance Engineering Journal 10:286-297.
36. Perlovich GL (2015) Thermodynamic characteristic of cocrystal formation and melting points for rational design of pharmaceutical two-component systems. Cryst Eng Comm 17:7019–7028.
37. Pessoa AS, Aguiar GPS, Oliveira JV, Bortoluzzi AJ, Paulino A, Lanza M (2019) Precipitation of resveratrol-isoniazid and resveratrol-nicotinamide cocrystals by gas antisolvent. J Supercrit Fluids 145:93–102.
38. Panzade P, Shendarkar G, Shaikh S, Rathi PB (2017) Pharmaceutical cocrystal of piroxicam : design, formulation and evaluation. Tabriz Univ Med Sci 7:399–408.
39. El-gizawy SA, Osman MA, Arafa MF, El Maghraby GM (2015) Aerosil as a novel co-crystal co-former for improving the dissolution rate of hydrochlorothiazide. Int J Pharm 478:773–778.
40. Yadav AV, Shete AS, Dabke AP, Kulkarni PV, Sakhare SS (2009) Co-crystals: a novel approach to modify physicochemical properties of active pharmaceutical ingredients. Indian J Pharm Sci 71:359-70.
41. Perlovich GL (2015) Thermodynamic characteristic of cocrystal formation and melting points for rational design of pharmaceutical two-component systems. Cryst Eng Comm 17:7019-7028.
42. Rustichelli C, Gamberini G, Ferioli V, Gamberini MC, Ficarra R, Tommasini S (2000) Solid-state study of polymorphic drugs: carbamazepine. J Pharm Sci 23:41–45.
43. Unsalan O, Erdogdu Y, Gulluoglu MT (2009) FT-Raman and FT-IR spectral and quantum chemical studies on some flavonoid derivatives: baicalein and naringenin. J Raman Spectrosc 40:562–570.
44. Brittain HG (2004) Fluorescence studies of the transformation of carbamazepine anhydrate form III to its dihydrate phase. J Pharm Sci 93:375–383.
45. Sarwar B, Kaisar R, Rajendra Kumar, Renu C, Katare OP, Bhupinder Singh (2016) Improved Intestinal Lymphatic Drug Targeting via Phospholipid Complexloaded Nanolipospheres of Rosuvastatin Calcium. *RSC Adv* 6:8173-8187.
46. Zhang GGZ, Law D, Schmitt EA, Qiu Y (2004) Phase transformation considerations during process development and manufacture of solid oral dosage forms. Adv Drug Del Rev 56(3):371-90.
47. Vemuri VD, Lankalapalli S (2019) Insight into Concept and Progress on Pharmaceutical Co-Crystals: An Overview. Indian J of Pharmaceutical Education and Research. 53(4s):s522-s538.
48. Dnyaneshwar P, KaleSandeep S, ZodeArvind K, Bansal (2017) Challenges in Translational Development of Pharmaceutical Cocrystals. J Pharm Sci 106:457- 470.

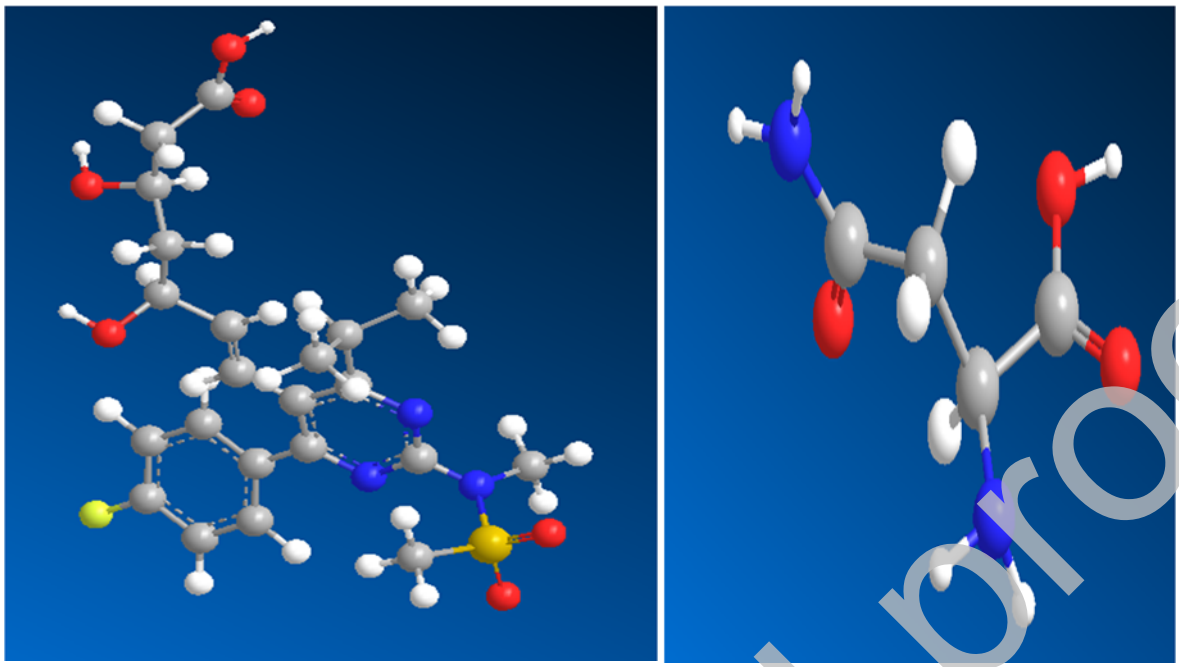

Fig. 1. Molecular structures of pure rosuvastatin calcium (RSC), L-asparagine (ASN)

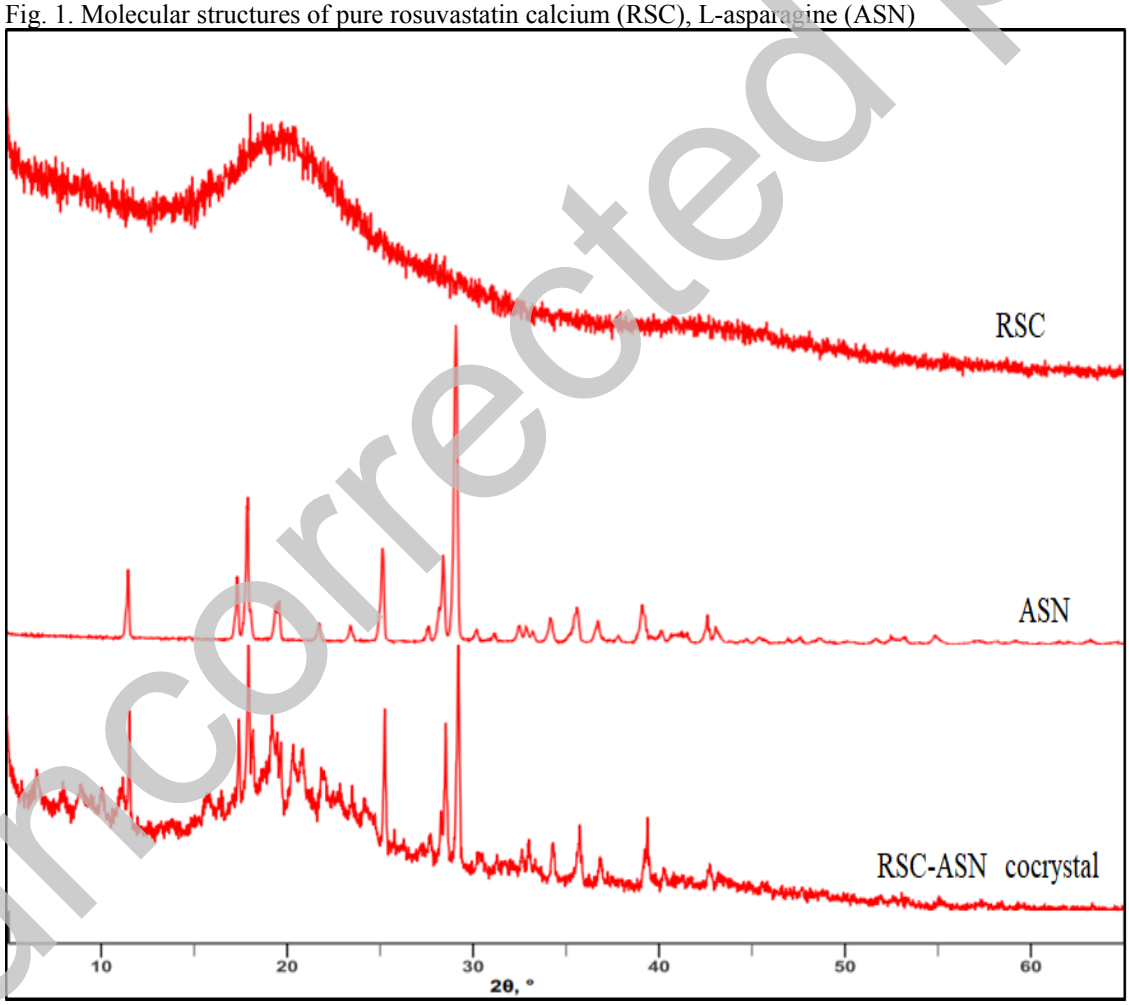

Fig. 2. Powder X-ray diffraction pattern of pure rosuvastatin calcium (RSC), L-asparagine (ASN) and rosuvastatin-asparagine (RSC-C) cocrystals.

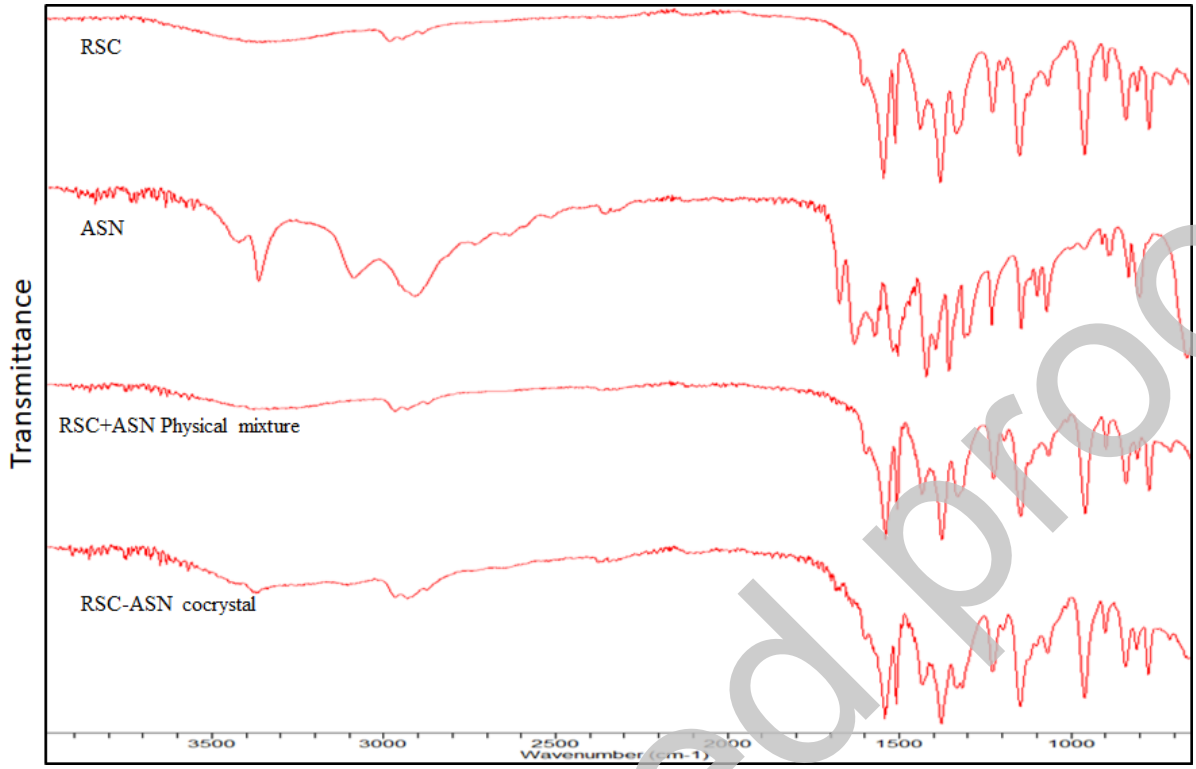

Fig. 3. FTIR spectra of pure rosuvastatin calcium (RSC), L-asparagine (ASN), rosuvastatin + asparagine physical mixture and rosuvastatin-asparagine (RSC-C) cocrystals.

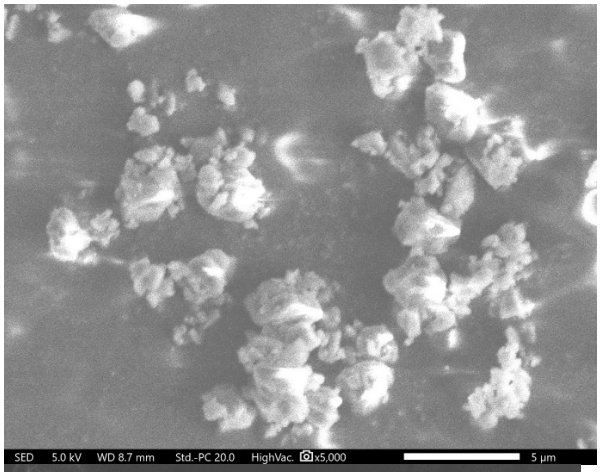

(A) (B)

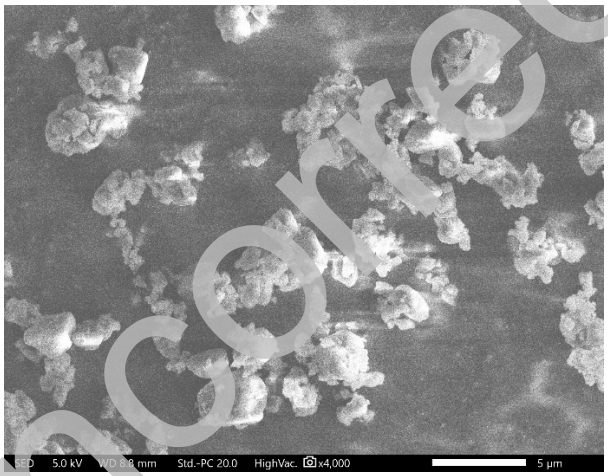

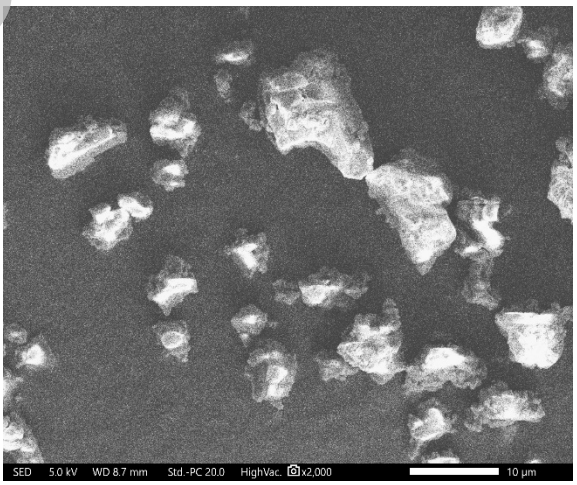

(C) (D)

Fig. 4. Field emission scanning electron microscopy (SEM) micrographs of (A)pure rosuvastatin calcium (RSC), (B) L-asparagine (ASN), (C) rosuvastatin + asparagine physical mixture, and (D)rosuvastatin-asparagine (RSC-C) cocrystals.

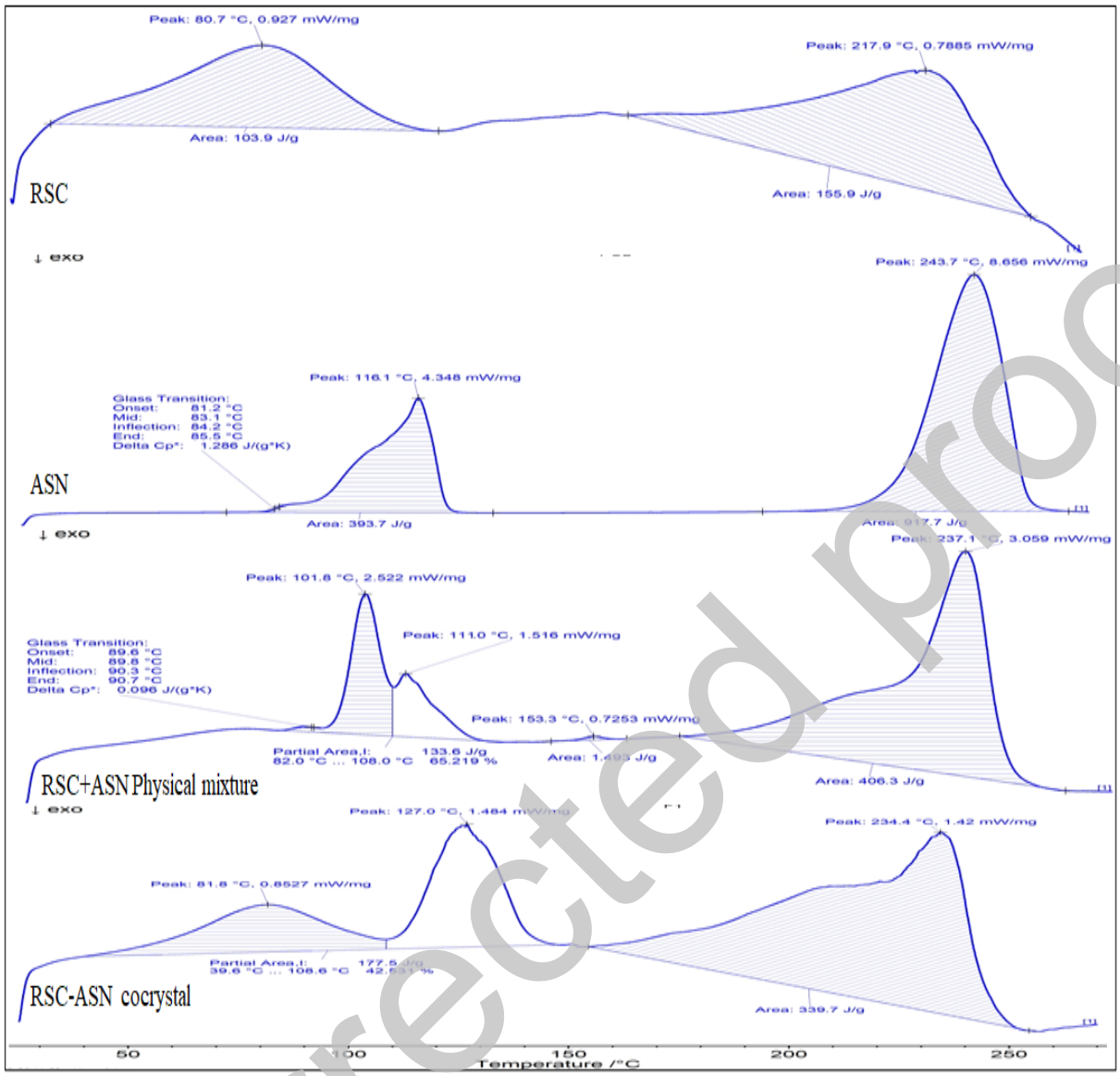

Fig. 5. DSC thermogram of pure rosuvastatin calcium (RSC), L-asparagine (ASN), rosuvastatin + asparagine physical mixture, and rosuvastatin-asparagine (RSC-C) cocrystals.

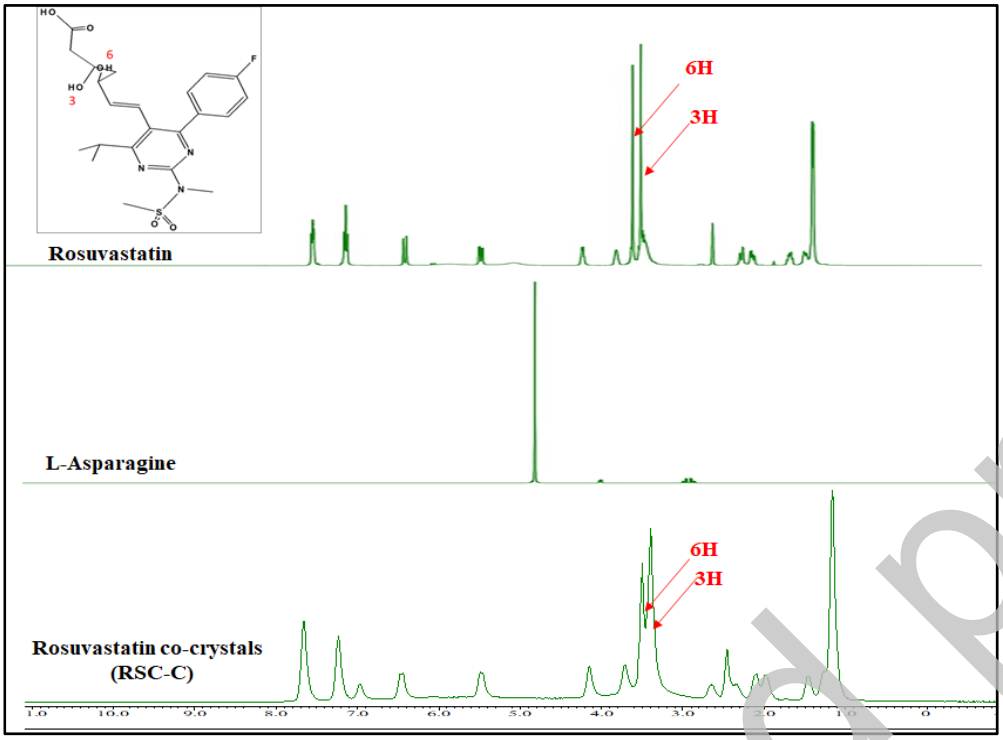

Fig.6. FT-NMR of pure rosuvastatin calcium (RSC), Co-former L-asparagine (ASN) and rosuvastatin-asparagine (RSC-C) cocrystals.

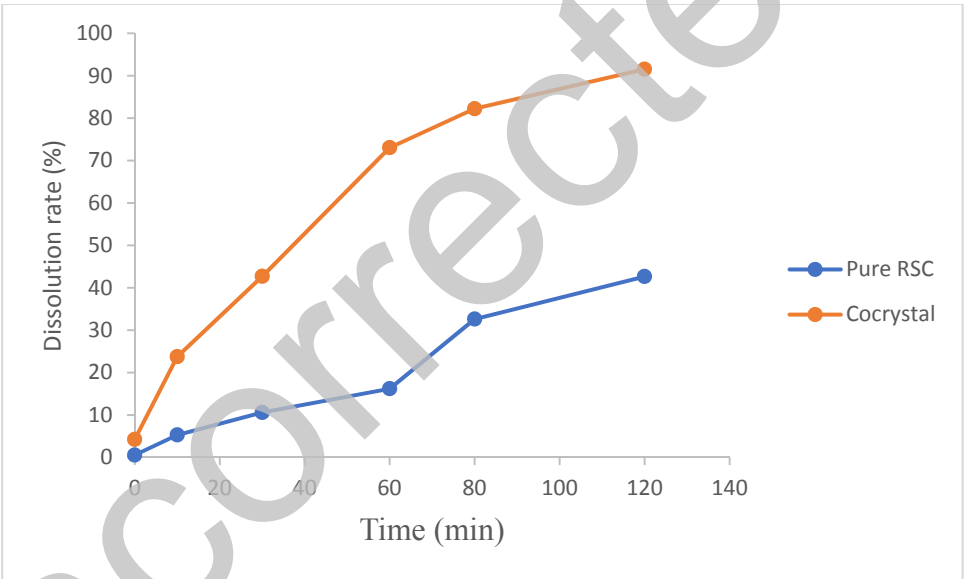

Fig. 7. Dissolution rate (%) of pure rosuvastatin calcium (RSC) and rosuvastatin-asparagine (RSC-C) cocrystals.

Table 1
Aqueous solubility of rosuvastatin calcium

Chemical moiety	*Solubility in water (mg/ml)*	*Solubility in pH 1.2 buffer (mg/ml)*	*Solubility in pH 4.5 buffer (mg/ml)*	*Solubility in pH 6.8 phosphate buffer (mg/ml)*
Rosuvastatin calcium	0.836±0.036	0.624±0.052	1.143±0.058	1.427±0.034
Rosuvastatin + L-asparagine physical mixture	0.948±0.052	0.745±0.078	1.236±0.034	1.247±0.042
Rosuvastatin-asparagine cocrystals	1.817±0.066	1.379±0.065	2.612±0.087	3.466±0.057

Mean ± SD, n=3

Table 2
Micromeritic evaluation of Cocrystals

Micromeritic evaluation	*Pure RSC*	*RSC-C Cocrystals*
Angle of repose (Ø)	32.31±0.56	2.81±0.45
Carr's index (%)	11.24±0.46	6.32±0.68
Hausner's ratio	1.18±0.21	1.06±0.02

Mean ± SD, n=3